Fluidization and Drying of Biomass Particles in a Vibrating Fluidized Bed with Pulsed Gas Flow

Dening Jia[a], Océane Cathary[b], Jianghong Peng[a], Xiaotao Bi[a]*, C. Jim Lim[a], Shahab Sokhansanj[a,c], Yuping Liu[d] and Ruixu Wang[a]

a. Department of Chemical and Biological Engineering, the University of British Columbia, 2360 East Mall, Vancouver, BC, V6T 1Z3, Canada

b. The ÉcoleNationaleSupérieure de Techniques Avancées, 828, Boulevard des Maréchaux, 92120,PalaiseauCedex, France

c. Environmental Sciences Division, Oak Ridge National Laboratory, Oak Ridge, TN 37831, USA

d. Collaborative Research Center for Energy Engineering, Institute of Industrial Science, The University of Tokyo, 4-6-1 Komaba, Meguro-ku, Tokyo 153-8505, Japan

Abstract

Fluidization of biomass particles in the absence of inert bed materials has been tested in a pulsed fluidized bed with vibration, with the pulsation frequency ranging from 0.33 to 6.67 Hz. Intermittent fluidization at 0.33 Hz and apparently 'normal' fluidization at 6.67 Hz with regular bubble patterns were observed. Pulsation has proven to be effective in overcoming the bridging of irregular biomass particles induced by strong interparticle forces. The vibration is only effective when the pulsation is inadequate, either at too low a frequency or too low in amplitude. Drying of biomass has been carried out to quantify the effectiveness of gas pulsation for fluidized bed dryers and torrefiers in terms of gas-solid contact efficiency and heat and mass transfer rates. The effects of gas flow rate, bed temperature, pulsation frequency and vibration intensity on drying performance ~~have been~~were systematically investigated. While higher temperature and gas flow rate are favored in drying, there exists an optimal range of pulsation frequency between 0.75 Hz and 1.5 Hz where gas-solid contact is enhanced in both the constant rate drying and falling rate drying periods.

I. Introduction

Biomass as a sustainable energy source has regained its popularity during the past decade, mainly attributable to the surging energy demand, supply shortage of fossil fuels, mitigation of greenhouse gases and the increasing public environmental awareness. The total energy supplied from biomass reached approximately 55.6×10^{18} J in 2013 [1] ? percent of the world energy production. The international trade of biomass has continued to grow considerably due to a higher demand, particularly for biofuels and wood pellets. Global production and transport of wood pellets already exceeded 23.6 million tonnes in 2013 [1], a 13% increase compared to 2012.

Despite the global ~~prosperity and~~ popularity of biomass, one of the major issues that hinder its further application is the high moisture content. Biomass from various sources generally contains high concentrations of water, which could be either free or chemically bonded. Sawdust directly obtained from sawmills contains over 60% of water, while in general ~~it should be controlled~~the moisture content must be reduced to ~~-~~under 13% as high moisture levels normally lead to energy losses, higher risks of mold formation during storage and decreased efficiency and increased emission in combustion. Studies have also shown that for biomass pelletization the ideal moisture content ranges from 5% to 15% on the dry basis [2].

~~There is no surprise that d~~Drying is an essential step for many biomass related operations such as pelletization. Research by Mani *et al.*[3] revealed that the cost of drying (capital and operation) alone could take up to 20% of the entire pelletization process while hammer mill and pellet mill combined share less than 10%. The energy consumption of biomass drying is approximately 2500-3000 MJ/tonne, whereas the grinding and pelletizing require only 400 MJ/tonne [3]. Therefore, in order to optimize pelletization in terms of process efficiency, energy consumption and product quality, not only it is important but also highly effective to focus on drying. Considering the current scale of operation for pelletization (up to 900,000 tonnes of pellets per year in a single pellet mill from sustainably managed forests [1]), even a small improvement in drying efficiency would significantly alter the outlook.

Compared to traditional biomass dryers (rotary drum dryer, conveyer belt dryer, etc.) fluidized bed offers excellent heat and mass transfer rates, uniform temperature distribution. However, the unconventional nature of biomass particles such as irregular shape, low bulk density and wide particle distribution has made biomass fluidization quite problematic [4]. The surface moisture on biomass materials increases the inter-particle forces dramatically [5], at several times bigger than the particle weight, which could lead to channeling, gas bypassing and eventually defluidization. Previous researchers introduced inert particles such as sand to the system to assist fluidization of biomass particles [6-9]. However, it increases ash content in biomass product due to attrition of inert materials, degrading the quality of biomass pellets and

subsequently posing serious problems to biomass-powered boilers and turbines that may as a result encounter corrosion, sintering, and slagging, which will require additional maintenance for the removal of deposits and even unscheduled shutdowns [10]. Therefore, fluidized bed dryers without the need of inert particles are greatly favored for drying biomass for the preparation of high quality feedstock (i.e. pellets).

Previous study by Liu *et al.* [11] showed the potential of fluidized bed drying of biomass without the aid of inert bed materials. Sawdust was dried in a 50 mm ID fluidized bed, the same one used by Li *et al.* [12], with acceptable gas-solid contact being achieved by the use of a novel distributor with vertically inclined orifices designed to increase radial particle movement.

Besides relying on improving the design of gas distributors and operated at high flow rates, pulsation and vibration have been commonly used in granulation, coating and drying of sticky powders and irregularly shaped agricultural products [13-27]. Pulsed fluidized beds, in which the gas flow rate oscillates periodically with time, have been proven effective in transforming random and chaotic bubble behavior into regular and ordered patterns, improving the fluidization quality of coarse particles greatly[28]. Similar to many mechanical systems, the behavior of pulsation is strongly linked to the frequency. Based on an analysis of one-dimensional particle motions in incompressible fluid, Molerus [29] interpreted the effect of vibration on the stabilization of particle fluidization, and concluded that 50 Hz was ~~a very~~an effective frequency in reducing gas bypassing. Similarly, Massimilla *et al.* [30] examined three types of pulsed fluidization at different pulsation frequencies, namely the intermittent fluidization at low frequencies (1.2 ~ 2.7 Hz), piston-like fluidization at medium frequencies (2.7 ~ 4.8 Hz) and an apparently 'normal' fluidization at high frequencies (>4.8 Hz). The piston-like behavior was not observed in experiments of Wong and Baird [31]. A mathematical model was proposed to offer approximate predictions of the natural frequency of the fluidized bed, around which the pulsation was most effective. DEM simulation by Wang and Rhodes [19, 32] confirmed that a frequency of 3 ~ 10 Hz be most effective in ameliorating gas-solid interaction. Periodically formed horizontal gas channels were spotted where they quickly gave rise to regular bubbles, which moved up to the surface of the bubbling bed.

Vibrated fluidized beds ~~bring~~ impart mechanical vibration energy into conventional fluidized beds to improve the fluidization quality of sticky and cohesive particles and to reduce the consumption of drying medium. Gupta and Mujumdar [33] discussed the hydrodynamics and heat transfer properties in vibrated fluidized beds and derived a power-type correlation for bed pressure drop at minimum fluidization velocity between vibrated and conventional fluidized beds. The promotion of heat and mass transfer rates in vibrated bed was confirmed by Eccles and Mujumdar [34], where the bed-to-surface heat transfer coefficient was measured in a vertically vibrated fluidized bed. By modifying the diffusion term in the conservation

equations for drying, Stakić and Urošević [14] successfully simulated drying of fine grains in both fixed and vibrated fluidized beds, and the simulation results were in agreement with the drying performance data obtained from vibrated fluidized beds. It was also found that vibrated beds had a shorter residence time and more uniform temperature distribution.

To improve the fluidization quality, i.e. achieving uniform drying, and gas-solids contact efficiency of fluidized beds of biomass particles for drying [11] and torrefaction [12], the effect of gas pulsation and bed vibration on the hydrodynamics and drying performance has been investigated in this study in a vibrating fluidized bed. Key parameters such as gas flow rate, bed temperature, pulsation frequency and vibration intensity have been investigated, which are crucial to the design and scaling-up of biomass dryers and torrefiers. Drying rate was adopted as a performance indicator for gas-solid contact efficiency and heat and mass transfer, which is crucial for the development of an energy-efficient fluidized bed reactor for biomass drying and/or torrefaction.

II. Experimental Setup

The pulsed fluidized bed with vibration (PVFB) is depicted in Fig 1. The fluidized bed column was made of Plexiglas with a rectangular cross-section (15 cm × 10 cm, and a height of 1.0 m). It was installed on a vibrating base (Eriez 48A, Eriez Manufacture Co., USA). The vibrating base had a constant frequency of 60 Hz and adjustable amplitude on a scale from 0 to 100%, corresponding to 0 to 0.381 mm of displacement. The drying medium was high-pressure building air. After being regulated by a pressure regulator (AR-40-N04H-Z, SMC, USA), the gas line branched out into two streams A and B. Both streams were equipped with a rotameter (FL6212-V and FL6213-V respectively, Omega, Canada) with needle valves to monitor and control the flow rate individually. The first stream A was the pulsating stream, on which a solenoid valve (8210G034-120/60, ASCO Valve, USA) was installed. The open and closing of the valve was controlled by a computer program. In order to reduce the fluctuation of gas flow rate through the rotameter, a surge tank was placed between the solenoid valve and the rotameter. The presence of the surge tank could also maintain a stable supply of drying air during operation. The second stream B was the fluidization stream where the flow rate of air was maintained constant. The purpose of this stream was to provide a stable gas flow to keep the bed mobilized. However, previous and preliminary studies have shown that at the same overall flow rate, the steady fluidization stream branched out from the same source of gas supply will dampen the 'shock' brought by the pulsation stream and undermine the positive effect of pulsation on the fluidization of biomass particles [35][S1]. Therefore, only the pulsation stream (Stream A) was used for the following experiments. The two streams merged before entering the inline gas heater (AHP-7561,

Omega, Canada) controlled by a temperature controller (CN4316, Omega, Canada) so that drying temperature could be regulated. A perforated aluminum plate with 1/8'' holes and 40% open area was used as gas distributor. A filter bag was installed at the exit of the column to retain the fines.

Figure 1. *Schematic drawing of the vibrated fluidized bed with pulsed gas flow*

Along the height of the column, there were six ports for temperature, relative humidity and pressure measurements. The first ~~one~~ port was located 25 mm above the gas distributor, and the others were 102 mm apart. Ports 1 and 5 were used to obtain pressure drop across the bed, through a pressure transducer (PX164-010D5V, Omega, Canada). The absolute pressure of the windbox (PX142-005D5V, Omega, Canada) and the column (PX163-005BD5V, Omega, Canada) were also monitored. Temperature in the windbox, dense phase and freeboard were measured by T-type thermocouples. Temperature and relative humidity of the gas phase at both inlet and outlet of the fluidization column were constantly monitored by humidity indicators (HMI41 at inlet, HMT335 at outlet, Vaisala, Finland). The analog signals of the pressure, temperature and the relative humidity were captured by data acquisition devices, so that ~~they~~ signals could be processed, visualized, and saved through Labview software (Version 2014, National Instrument, USA) onto a PC. Labview was also used to control the solenoid valve through a digital output channel. The specific devices used and sampling rate of the signals are listed in Table 1 below. A high-speed camera (1280× 720 pixel, f/2.2 aperture, 240 frames per second) was mounted in front of the Plexiglas column to capture the transient behavior of the fluidized bed.

Table 1. *Summary of data acquisition device and acquired signals*

Biomass material used in this study, Douglas fir and pine sawdust, was generously donated by Tolko Industries Ltd (Vernon, Canada). Switchgrass was also used. The raw materials were passed through a 3.5 mm sieve to ~~get rid of~~remove larger particles unsuitable for fluidization. Particle size distributions after sieving are shown in Fig. 2. Switchgrass has more fines, while pine and fir contain more coarse particles (1.7 mm ~ 3.5 mm). Other basic properties including Sauter mean diameter, bulk and true densities, as well as sphericity are listed in Table 2. True density was measured by a multi-pycnometer (Quantachrome Instruments Co. Florida, USA), and sphericity was measured by an image processing software developed in ~~this group~~house at the University of British Columbia [42]. All biomass materials were sun-dried and stored in cold room to prevent microbial activities[S2].

To investigate suitable operating parameters for biomass drying in terms of flow rate, pulsation frequency and duty cycle, vibration intensity, air temperature ~~etc.~~, batch-wise drying tests were conducted in the PVFB. Samples in each set of the experiment were prepared together and therefore have the same moisture content, which was controlled around 65%. 200 g of sample was placed into the fluidized bed and dried for 30 min.

Since the moisture contents at the inlet and outlet were constantly monitored, combined with known flow rate, pressure and temperature, the drying rate R_w was obtained by,

$$R_w = \frac{dw}{dt} = M \cdot (Y_{out} - Y_{in}) \quad (1)$$

Where M is the mass flow rate, Y_{out} and Y_{in} are the ~~specific~~ absolute humidity, which is the mass ratio of water vapor to dry air, calculated by,

$$Y = 0.622\left(\frac{p_s}{p - p_s}\right) \quad (2)$$

p_s is the water vapor saturation pressure, obtained from the Wagner-Pruss equation [36],

$$\ln\left(\frac{p_s}{22.064\times10^6}\right) = \frac{647.096}{T}(-7.85951783\nu + 1.84408259\nu^{1.5} - 11.7866497\nu^3 + 22.6807411\nu^{3.5} - 15.9618719\nu^4 + 1.80122502\nu^{7.5}) \quad (3)$$

in which

$$\nu = 1 - \frac{T}{647.096} \quad (4)$$

T is the air temperature in Kelvin. In addition, the instantaneous drying rate could be calculated directly in Labview with equations provided above.

Figure 2. *Particle size distribution of bed materials*

At the end of each drying test, a small sample of biomass particles was ~~also~~ collected. Together with the wet particles, the moisture contents of all samples were determined according to the ASTM D4442-07 standard by heating the samples at 103 °C for 24 h in a precision oven. The sample moisture content (dry basis, w% d.b.) is calculated by

$$X_{d.b} = \frac{m_{wet} - m_{dry}}{m_{dry}} \times 100\% \quad (5)$$

Where m_{wet} and m_{dry} are the weight of moisture of the sawdust samples before and after drying. Final moisture contents of biomass samples are normalized so that results from different experiments can be better compared. Moisture ratio MR is defined as follows,

$$MR = \frac{X - X_e}{X_o - X_e} \times 100\% \quad (6)$$

With X_o being the initial moisture content, X_e the equilibrium moisture content in a sample. In this work the equilibrium moisture content was 4% ~ 8% (referenc), which is relatively small compared to X_o, MR is then simplified to,

$$MR = \frac{X}{X_o} \times 100\% \quad (7)$$

Similarly, the drying efficiency η, or the efficiency of water removal could be defined as,

$$\eta = \frac{X_o - X}{X_o} \times 100\% \quad (8)$$

III. Experimental Results

3.1 Hydrodynamics in fluidized bed dryer

3.1.1 Pressure Fluctuations

In the case of pulsed fluidized bed with biomass particles, the relatively chaotic nature of the bed is structured by the external excitation caused by the pulsed gas flow [28]. For instance, at 0.33 Hz, each pulsation cycle consists of the solenoid valve being opened for 1.5 seconds and closed for 1.5 seconds, as a result the gas ~~phase~~ is introduced to the fluidized bed every 3 seconds. ~~periodically.~~ Distinct 'Flow-On' and 'Flow-Off' period were observed. As can be seen from Fig. 3 (a) each 'On' period starts with a dominant peak of bed pressure drop (marked with letter A[S3]), corresponding to the onset of gas flow immediately after the solenoid valve was switched open. The major peak is followed by a decaying oscillation (B - C). The uprising gas bubbles mixing with falling particles may have contributed to the oscillatory pressure profile from points B to C. At the end of each 'On' period there is also a brief pressure recovery (C – D) caused by falling particles compressing the gas phase in the plenum chamber. The bed remained stationary during 'Off' period due to the lack of gas supply, the pressure profile flat lines (D - E). Similar pattern could be seen at 1 Hz in Fig. 3(b), with F representing the dominant peak and G – H the pressure oscillation. It should be noted that at lower pulsation frequencies, the intensity of the pulsation is greater, which leads to longer period of decaying oscillations. Five or more peaks can be identified during the decaying oscillation at 0.33 Hz, while only one is observed at the relatively low-intensity at 3 Hz. As the pulsation frequency keeps increasing, particles will be carried up by gas phase from the next cycle before reaching the bottom of the fluidized bed. Consequently, the pressure goes up before it could start

oscillating, which explains the disappearance of decaying oscillation altogether at 6.67 Hz, as illustrated in Fig. 3(d).

Figure 3. *Pressure fluctuations in PVFB at various pulsation frequencies*

3.1.2 Gas-solid Flow Behavior

Typical flow behavior of the pulsed fluidized bed at various pulsation frequencies are shown in Fig. 4. Average gas velocities in all experiments were kept constant and high enough to avoid severe channeling and gas bypassing. At the lower end of all pulsation frequencies investigated in this work such as 0.33 Hz, the bed was fluidized intermittently due to prolonged 'On' and 'Off' period in each pulsation cycle. The bed remained stationary during the 'Off' period while sufficiently high pressure had built up in the surge tank. As soon as the solenoid valve was opened, pressurized gas stored in the surge tank would be quickly discharged into the fluidized bed. Chains of slugs were formed above the distributor, denoted by the yellow rectangle in Fig. 4 (A1).The frequency of slug formation remained identical to the pulsation frequency. Slugs quickly rose to the top of the bed via a few channels (A2), while the remaining gas in this cycle kept mixing with biomass particles (A3). The high intensity of gas pulsation at 0.33 Hz was powerful enough to lift the entire bed, therefore the amplitude of bed expansion reached a maximum with heavy elucidation. A large amount of fines was collected in the bag filter. As the pressure of the gas phase diminished and solenoid valve closed, particles eventually fell back to the bed (A4), which remained stationary until the next cycle.

The interval between two gas injections became shorter at 1 Hz. The horizontal layer of slugs (B1) quickly evolved into gas channels that zigzagged up the bed, as is shown in Fig. 4 (B2) and (B3). The bed expanded slightly less due to reduced pressure build-up and gas velocity. No regular bubble flow pattern could be seen at this frequency due to the cohesiveness of particles and high intensity of pulsation. However, at 3Hz the horizontal slugs (C1) quickly gave rise to large bubbles (circled in Fig. 4 C2 and C3). The 'Off' period disappeared as the pulsation frequency exceeded the natural frequency of the fluidized bed, particles were lifted up again before it could reach the bottom of the bed. This is consistent with the disappearance of decaying pressure oscillation shown in Fig. 3 (c). At 6.67 Hz, the peak instantaneous gas velocity in each pulsation cycle was much smaller than that at 0.33 Hz. There was a stronger resistance from particles to prevent the formation of bubbles. The combined effect of faster gas renewal and less excessive gas available to bubble formation led to the reduction in bubble size and bed expansion. Shown in Fig. 4 (D1), slugs formed at 6.67 Hz quickly disappeared and split into regular bubbles (circled in Fig. 4 D2, D3). The pulsed fluidized bed at this frequency behaved like a conventional fluidized bed if the biomass particles were able to be fluidized under similar conditions.

Figure 4. *Typical fluid patterns of the bed at various pulsation frequencies. A1-A4 Pulsation frequency = 0.33Hz, B1-B4 1Hz, C1-C4 3Hz, D1-D4 6.67Hz*

Fast Fourier Transform (FFT) analysis was ~~also~~ performed on the pressure signals (Fig 5?). Similar to a conventional fluidized bed where the power spectrum of pressure fluctuations reflects bubble frequency, including bubble formation, splitting and coalescence, the dominant frequency in pulsed fluidized bed corresponds to the pulsation frequency, as shown in Fig. ~~6~~5. Peaks are more distinct for the pulsed fluidized bed, and several orders of magnitude higher than that of a conventional fluidized bed[S4]. The appearance of overtones of the dominant frequency could be attributed to the under-dampened pressure oscillations, and the fact the pressure fluctuations in pulsed fluidized bed are not perfect sinusoids[S5].

3.1.3 Effect of Moisture Content on Hydrodynamics

The hydrodynamics of the PVFB relates closely to the moisture content of biomass particles. Water will form bridges between particles, introducing capillary liquid bridge forces, which are consisted of the surface tension force and the force caused by the pressure difference outside and inside the bridge[S6]. As the particles are being dried, moisture is consistently being removed. The liquid bridge force will change, as a result, which affects the hydrodynamics of the fluidized bed significantly[S7]. The relationship between moisture content and pressure fluctuations is especially important. Fig. 6 presents the time-averaged standard deviation of pressure fluctuations at various pulsation frequencies during the batch drying process. Similar to conventional fluidized beds, the standard deviation of pressure fluctuations is mainly associated with bubble size. It is obvious that the highest amplitude of pressure fluctuations exhibits at 0.33 Hz, and decreases with increasing pulsation frequency. This is consistent with visual observations obtained during the drying tests. At lower pulsation frequencies, larger voids and bed expansion are observed. The standard deviation also decreases during drying, indicating the bubble size reduces as the particles are being dried. This may have been caused by the breaking down of liquid bridges between particles, as the bubbles are less inhibited by such cohesive forces from splitting up.

Figure 5. *Spectrum analysis of pressure fluctuations at various pulsation frequencies*

Figure 6. *Standard deviation of pressure fluctuations at various pulsation frequencies*

3.2 Drying in Vibrated Fluidized Bed with Pulsed Gas Flow

3.2.1 Effect of Gas Flow Rate

Gas flow rate has a direct impact on drying. Unlike conventional fluidized beds, pulsed fluidized beds could be operated at an average gas velocity lower than the minimum fluidization velocity. In this work U_{mf} was[S8] calculated according to Cui and Grace [37]. For Douglas fir samples used in this study,

$U_{mf} = 0.238$ m/s. Successful fluidization was achieved with an average gas velocity as low as $0.8U_{mf}$, combined with a strong pulsations at 0.33 Hz or 0.5 Hz. As the pulsation frequency increases, higher gas velocity is required to maintain good gas-solid contact. $1.2\ U_{mf}$ was found to be sufficient for pulsations up to 6.67 Hz. Fig. 7 depicts the moisture ratio *MR* of the Douglas fir sawdust after 30 min of drying at various gas flow rates. Since 200 g of Douglas fir samples with the same initial moisture content were placed into the fluidized bed before each run, a low moisture content at the end of drying, or X/X_o, would suggest a faster drying and subsequently a better gas-solid contact. Certain experiments were repeated three times, and good repeatability was obtained. A higher average gas velocity seemed to lead to a higher drying efficiency. For 0.5 Hz and 3 Hz pulsation, as the average superficial gas velocity increased from $1.5U_{mf}$ to $2U_{mf}$, the moisture ratio *MR* decreased by 8.4% and 13.8% respectively. In addition, it appears that for dryers that ~~is~~ are being operated at a moderate flow rate ($1.2U_{mf} \le \bar{U} < 1.9U_{mf}$), higher pulsation frequency is favored. In the case of very low ($<1.2U_{mf}$) or very high ($>1.9U_{mf}$) flow rates, a lower pulsation frequency is preferred[S9].

Figure 7. *Effect of flow rate on the final moisture content of Douglas fir sawdust after 30 min of drying*

3.2.2 Effect of Pulsation Frequency

As a crucial parameter in pulsed fluidized beds, the impact of pulsation frequency on drying has been investigated and is given in Fig. 8. Due to the limitations of the solenoid valve, the maximum pulsation frequency investigated in this study was 6.67 Hz. Since the velocity profiles at various pulsation frequencies are different, it is important that the average gas velocities be kept the same to ensure the comparability of the results. Two average superficial gas velocities were studied, $\bar{U} = 0.8U_{mf}$ and $\bar{U} = 1.3U_{mf}$.

Figure 8. *Effect of pulsation frequency on the final moisture content of Douglas fir sawdust after 30 min of drying*

With the relatively high velocity of $1.3U_{mf}$, the bed could be successfully fluidized at a wider range of pulsation frequencies compared to $0.8U_{mf}$. No severe channeling or gas bypassing that could hinder the drying process was observed from 0.33 Hz to 6.67 Hz. The moisture ratio dropped from 19.3% at 0.33 Hz to 14.5% at 6.67 Hz as shown in Fig. 8, indicating that an increase in pulsation frequency was favored during drying. The situation was completely different once the gas velocity was lowered. For $\bar{U} = 0.8U_{mf} < U_{mf}$, channeling was observed at approximately 3.5 Hz and above. Gas phase bypassed the particles and traveled through the channels with negligible gas-solid contact, which explained the dramatic decrease in the drying

efficiency at 3.3 Hz and 5 Hz. No channeling was observed below this frequency, as the pulsation was strong enough to overcome the cohesiveness of biomass particles. However, the prolonged 'Off' period at 0.33 Hz and below hindered drying, causing the final moisture content in biomass samples to increase slightly, from 22.4% at 0.75 Hz to 25.3% at 0.33 Hz. This made 0.75 ~ 1.5 Hz among the most effective frequencies for drying, a sweet spot for the operation of pulsed fluidized bed dryers of current configuration.

3.2.3 Effect of Vibration Intensity

Similar drying tests were carried out to verify the contribution of vibration to the fluidization of biomass particles. Two gas velocities were used, with the amplitude of vibration set to 0%, 25%, 75%, 50% and 100%. Similar to previous tests, the final moisture ratio (X/X_0) of biomass samples after 30 min of drying was also chosen as an indicator of fluidization quality.

Figure 9. *Effect of vibration intensity on drying, Douglas fir sawdust under 1 Hz pulsation frequency*

It is obvious that biomass dries faster at a higher gas velocity of $\bar{U} = 1.3U_{mf}$ compared to $0.8U_{mf}$, as shown in Fig. 9. A minimum of 17.8% difference in moisture ratio could be seen between the two gas flow rates. At $0.8U_{mf}$, a reduction in channeling and gas bypassing was observed in the fluidized bed immediately after the vibration was turned on. It appears that even a low vibration intensity of 25% is sufficient to overcome the cohesive forces between biomass particles. Consequently, the final moisture content decreased by 7% compared to the case where no vibration was applied. Higher amplitudes yielded only marginal improvement. In the case of $1.3U_{mf}$ where pulsation is capable of overcoming the inter-particles forces, the contribution of vibration is less obvious. Less than 2% of difference in moisture ratio suggests that pulsation alone should be enough to handle biomass particles, provided that suitable operating conditions are implemented.

3.2.4 Effect of Temperature

Series of drying test were conducted at different air temperatures to investigate the effect of temperature on drying rates. Limited by the Plexiglas column, temperatures up to 50 ℃ were tested. The fluidized bed column was pre-heated to designated temperatures for 30 min prior to any drying tests. Despite the pulsating nature of the gas flow, temperature of the inlet air could be controlled within 0.5 ℃. Fig. 10 demonstrates the effect of temperature on drying of Douglas fir sawdust at various pulsation frequencies. All three curves possess similar trends, as higher temperature does promote dying rate. One third of the experiments were

repeated three times to ensure credibility of the results, the standard errors were[S10] less than 1 %. For 0.33 Hz, the final moisture ratio of Douglas fir samples after 30 min of drying decreased from 44.2 % to 10.4% as the temperature rises from 20 ℃ to 50 ℃, consequently the drying efficiency η improves by 33.8%. At 1 Hz and 3 Hz, the moisture ratio decreased by 24% and 21% respectively. In the case of drying porous particles, temperature affects both external and internal conditions of drying. Higher temperature will speed up the evaporation of free water on the surfaces of biomass particles, which leads to faster drying in the constant rate period. In the falling rate period where heat conduction from the surface to the core of a particle is important, higher gas temperature will increase the temperature gradient between particle surface and core, leading to faster transfer of bound water from core to surface and evaporation at the surface. Little difference in moisture ratio can be found for pulsation at 1 Hz and 3 Hz at 50 ℃, indicating that gas velocity/external mass transfer may have become the rate-controlling step here.

Figure 10. *Effect of temperature on the drying of Douglas fir sawdust at various pulsation frequencies, $U/U_{mf}=1.25$*

3.3 Drying Mechanisms

Typical drying curves for all three biomass species including Douglas fir, pine and switchgrass[S11] are shown in Fig. 11(a). Since pre-conditioned wet particles were loaded into the fluidized bed dryer prior to each run, some surface moisture on the wet particles evaporated and cumulated in the freeboard[S12] region. Therefore, it is highly likely that the fast decline of drying rate during the first 5 min is caused by the removal of cumulated moisture from the freeboard by introduced dry air and should be excluded from the analysis. In addition, the samples have a slightly higher temperature than the drying air in this set of experiments (~ 5 ℃), which could also contribute to the higher drying rates as higher temperature promotes drying. The constant rate drying is reached after the initial system response, as indicated by the constant relative humidity of the exhaust gas. At this stage, a thin film of water covers the surface of particles, on which the evaporation mainly takes place. The rate of drying is limited by the evaporation of water, which could be characterized as a heat-transfer limited process, only to be influenced by external conditions such as temperature, humidity and flow rate of the drying air.

Figure 11. *Typical drying curves of three biomass species (a) Drying rate vs. time (b) Bed temperature vs. time*

Bed temperature remains constant during constant rate drying. However, as drying proceeds, dry spots appear on the surface of particles once critical moisture content is reached. Although drying rate per unit wet area remains the same, a reduction in wet areas causes the drying rate to decline. As the surface of the particles completely dries out, surface temperature increases significantly. Drying becomes a mass-transfer

limited process that is mainly driven by the concentration gradient between the core and surface of the particles. Temperature profiles during drying are illustrated in Fig. 11(b), in which three distinct areas could be identified, representing two drying mechanisms. The initial temperature drop is most likely caused by the evaporation of water removing heat from the bed of particles.

IV. Discussion

As shown in the previous section, pulsed fluidized beds could be operated below minimum fluidization velocity with reasonable heat and mass transfer rates for biomass drying, leading to potential savings in drying medium consumption. Fig. 8 shows that operating the fluidized bed at $\bar{U} = 0.8U_{mf}$ with 0.75 Hz pulsation, the remaining moisture content in the biomass sample after 30 min of drying is only 5% higher than that operated at $1.3U_{mf}$ with the same frequency. Higher or lower pulsation frequency than 0.75 Hz reduces the drying efficiency at $\bar{U} = 0.8U_{mf}$, while at $\bar{U} = 1.3U_{mf}$ the drying efficiency monotonically increases with increasing the pulsation frequency. One of the possible explanations is provided in Fig. 12, which demonstrates two gas velocity profiles in the pulsed fluidized bed, $\bar{U} < U_{mf}$ and $\bar{U} > U_{mf}$. Although theoretically the velocity profile should be square waves, in reality due to the actuation time of the solenoid valve (less than 1 second) and the damping of the flow through the pipe and plenum chamber, they are closer to sinusoidal waves. The gas phase is only capable of lifting the biomass particles when it possesses enough kinetic energy, i.e. when instantaneous gas velocity is higher than minimum fluidization velocity ($U > U_{mf}$). In each pulsation cycle there is a certain period of time that satisfies this condition. These periods are marked as 'fluidized zones' in Fig. 12, with their duration depending on the pulsation frequency and the average flow rate. Fig. 12 (a) represents a typical scenario where $\bar{U} > U_{mf}$. Of the two frequencies portrayed in this figure, 1.5 Hz possesses a longer period of time in which $\bar{U} < U_{mf}$ within each cycle compared to 4.5 Hz. This suggests that increasing the pulsation frequency from 1.5 Hz to 4.5 Hz will give rise to a larger portion of time in each cycle where the gas phase is powerful enough to fluidize the particles. This explains the decreasing moisture ratio with increasing pulsation frequency at $\bar{U} = 1.3U_{mf}$. Situation is reversed for $\bar{U} < U_{mf}$ when most of the gas flow in a pulsation cycle is too weak to overcome the bridging forces in the fluidized bed, leaving most effective drying carried out in a limited period of time. A higher pulsation frequency wakens the pulsation amplitude, with less portions of gas velocity exceeding U_{mf} in

each cycle. This is consistent with the observation that only at lower pulsation frequencies could the bed be effectively fluidized when $\bar{U} = 1.3U_{mf}$. On the other side of the spectrum however, an extremely low pulsation frequency brings no benefits either. For instance, 0.33 Hz will leave the bed stationary for 1.5 seconds, providing enough time for the formation of particle bridges again, which further indicates that too high or too low frequencies are equally detrimental to the drying of biomass when $\bar{U} < U_{mf}$.

Figure 12. *Schematic drawing of the pulsations at different frequencies and flow rates*

Besides the intensity of pulsation at different frequencies, the inherent nature of the fluidized bed may have affected the drying rate as well. It has been demonstrated that gas-solid fluidized beds could be characterized as a second-order mechanical vibration system, in which the pressure waves represent the output response of such a dynamic system to an external excitation [38], and the under-damped natural frequency f_n could be expressed as,

$$f_n = \frac{1}{2\pi}\sqrt{\frac{g}{H_{mf}}} \tag{9}$$

where H_{mf} is the bed height of the fluidized bed. Pressure fluctuations in fluidized beds could be originated from the passage of bubbles near a pressure transducer, oscillations of the bed surface, the plenum chamber, or even the gas blower [39-41]. In the pulsed fluidized bed, the pressure fluctuations are mainly initiated by the gas pulsation. As illustrated in Fig. 5 with the power spectrum analysis, the dominant frequency of the pressure fluctuations in a pulsed bed equals the frequency of the gas pulsation. The pressure waves are normally dampened as they travel through the fluidized bed due to inter-particle collision, relative motion between the interstitial gas and the particles, as well as the particle-wall friction. By incorporating the damping factor, ζ, the natural frequency is then rewritten as,

$$f_n^{'} = \frac{\sqrt{1-\zeta^2}}{2\pi}\sqrt{\frac{g}{H_{mf}}} \tag{10}$$

Since the fluidized bed is mostly an under-dampened system, ζ is then less than 1, with typical values reported in the literature being around 0.3 [38]. Most previous studies on the dampening of pressure waves were conducted in fluidized beds where particles with controlled size and shape were used. Neither the damping of pressure waves in pulsed fluidized beds, nor the change of damping factor with the moisture

content of particles has been investigated. By measuring the amplitude of the first and second peak of the pressure waves in each pulsation cycle (e.g. amplitudes of peaks A and B, Fig. 3), damping factor ζ could be calculated. Fig. 13 provides the change in damping factor during a typical batch drying process. Evidently, 0.33 Hz possesses a higher damping factor than 1.0 Hz, which is consistent with the findings of Roy *et al.* [41] that the damping effect was proportional to the intensity of the excitation signals. At both pulsation frequencies, the damping factor decreases as drying progresses, indicating the dampening of pressure waves is associated with the change in particle moisture content, or more precisely the inter-particle forces. In the beginning of each drying test, biomass contains very high moisture content that has made the particles particularly cohesive. Channeling and gas bypassing occurs, causing most of the energy being dissipated as a large portion of the gas phase goes through the fluidized bed without contacting the solids. Consequently, the damping factors are very high at the beginning, $\zeta = 0.70$ for 0.33 Hz, and $\zeta = 0.50$ for 1.00 Hz pulsation. As drying continues, moisture is being removed, the capillary force reduces significantly. The bed becomes free-flowing rather than channeling, and the relative motion between gas and particles is enhanced. As more kinetic energy is being absorbed by the particles, the damping factor decreases. Moreover, the higher-than-normal damping factor observed in the pulsed fluidized bed reveals the unconventional nature of biomass particles that often cause difficulties in fluidization. By introducing pulsation, the gas-solid and inter-particle interactions are promoted due to the intermittent acceleration and deceleration of particle movement.

Figure 13. *Damping factor of the pulsed fluidized bed during drying of biomass*

Based on the experimentally obtained damping factor of $\zeta = 0.2$~0.7, the natural frequency of the pulsed fluidized bed in this study is calculated to be 0.92 ~ 1.54 Hz according to Eqn. (10). As the dominant frequency of the system approaches its natural frequency, resonance will occur in the fluidized bed just like in a mechanical system, which will result in higher amplitude of pressure fluctuations as well as improved gas-solid contact. This may have contributed to the fact that the highest drying efficiency for $\bar{U} < U_{mf}$ is at 0.75 Hz, which is close to the natural frequency of the pulsed fluidized bed. As the pulsation frequency departs from the natural frequency, the drying efficiency decreases.

V. Conclusions

Pulsed fluidized bed with optional assistance of vibration has proven to be effective in fluidizing various biomass materials such as Douglas fir, pine and switchgrass, demonstrating that pulsed fluidized bed is a versatile and highly potential candidate for biomass torrifiers[S13]. The gas-solid flow behavior at different pulsation frequencies was analyzed. The fluidized bed is only fluidized intermittently below 3 Hz with slugs forming above the distributor that quickly give rise to gas channels. Large bubbles are formed at 3 Hz instead of channels, above which regular bubble patterns could be observed. At even higher pulsation frequencies, the pulsed fluidized bed behaves similar to a conventional one.

Dying test results indicated that temperature and gas velocity played a significant role in biomass drying, as they both were able to boost the mass transfer rate from surface of the particles to the drying medium. Higher temperature and flow rates usually lead to faster drying. Pulsation frequency, on the other hand, influenced the hydrodynamics and tied closely with the natural frequency, as well as the flow regime. The frequency between 0.75 Hz and 1.5Hz with the average gas-velocity right below minimum fluidization velocity seems to be a good spot, offering comparable drying performance at much higher gas flow rates. Vibration was found to be useful for fluidizing cohesive particles, especially when the extra acceleration brought by gas pulsation is not sufficient to break up the interparticle forces. However, when pulsation is sufficient in overcoming the cohesiveness of biomass particles, vibration will become unnecessary.

Drying characteristics over 30 minutes drying period was also studied. Two major mechanisms were identified during the drying of all three species of biomass, namely the constant rate drying and falling rate drying. However, due to the placement of the humidity indicator, a system delay contributed to the decline in the drying curve prior to the constant rate drying section. Further investigation of the relationships between certain parameters during drying, for example drying rate vs. bed pressure fluctuations, or bed temperature vs. average cycle frequency is essential for further advancing the knowledge of the intricate relationships between hydrodynamics and biomass drying performance.

Acknowledgment

The authors are grateful for the financial support provided by the Natural Sciences and Engineering Research Council of Canada (NSERC), as well as Tolko Industries Ltd. for the generous donation of tested biomass samples.

Nomenclature

f_n	Natural frequency of the fluidized bed, Hz
$f_n^{'}$	Modified natural frequency of the fluidized bed, Hz
g	Gravitational acceleration, m/s^2
H_{mf}	Static bed height, m
m_{wet}	Water content in wet biomass samples, g
m_{dry}	Water content in dried biomass samples, g
M	Mass flow rate of drying air, g/s
MR	Moisture ratio
p	Water vapor pressure, Pa
p_s	Saturated water vapor pressure, Pa
R_w	Drying rate, g/s
t	Time, s
T	Temperature, K
U	Instantaneous gas velocity, m/s
$\bar{U}$	Average gas velocity, m/s
U_{mf}	Minimum fluidization velocity, m/s
w	Weight of the sample, g
X	Moisture content of biomass samples, dry basis
X_o	Initial moisture content of biomass samples, dry basis
Y	~~Specific~~ Absolute humidity, g-water/kg-air

Greek Letters

η	Drying efficiency
v	Simplified term, K^{-1}
ξ	Damping factor

References

[1] R. Secretariat, Renewables Global Status Report, REN21, Paris, 2014.
[2] R. Renström, J. Berghel, Drying of Sawdust in an Atmospheric Pressure Spouted Bed Steam Dryer, Drying Technology, 20 (2002) 449.
[3] S. Mani, S. Sokhansanj, X. Bi, A. Turhollow, Economics of Producing Fuel Pellets from Biomass, Applied Engineering in Agriculture, 22 (2006).
[4] R. Legros, C. Alan Millington, R. Clift, Drying of tobacco particles in a mobilised bed, Drying Technology, 12 (1994) 517-543.
[5] J.P.K. Seville, C.D. Willett, P.C. Knight, Interparticle forces in fluidisation: a review, Powder Technology, 113 (2000) 261-268.
[6] S.M. Tasirin, I. Puspasari, A.W. Lun, P.V. Chai, W.T. Lee, Drying of kaffir lime leaves in a fluidized bed dryer with inert particles: Kinetics and quality determination, Industrial Crops and Products, 61 (2014) 193-201.
[7] M.J.C. van der Stelt, H. Gerhauser, J.H.A. Kiel, K.J. Ptasinski, Biomass upgrading by torrefaction for the production of biofuels: A review, Biomass and Bioenergy, 35 (2011) 3748-3762.
[8] H.J. Ciro-Velásquez, R.L. Cunha, F.C. Menegalli, Drying of Xanthan Gum Using a Two-Dimensional Spouted Fluidized Bed (2DSFB) with Inert Particles: Performance and Rheological Considerations, Drying Technology, 28 (2010) 389-401.
[9] R. Moreno, G. Antolín, A. Reyes, Quality of Fluidisation for the Drying of Forestry Biomass Particles in a Fluidised Bed, Biosystems Engineering, 94 (2006) 47-56.
[10] J.H. Turnbull, Use of biomass in electric power generation: the california experience, Biomass and Bioenergy, 4 (1993) 75-84.
[11] Y. Liu, J. Peng, Y. Kansha, M. Ishizuka, A. Tsutsumi, D. Jia, X.T. Bi, C.J. Lim, S. Sokhansanj, Novel fluidized bed dryer for biomass drying, Fuel Processing Technology, 122 (2014) 170-175.
[12] H. Li, X. Liu, R. Legros, X.T. Bi, C.J. Lim, S. Sokhansanj, Torrefaction of sawdust in a fluidized bed reactor, Bioresource technology, 103 (2012) 453-458.
[13] C. Liu, L. Wang, P. Wu, F. Xiang, Size distribution in gas vibration bed and its application on grain drying, Powder Technology, 221 (2012) 192-198.
[14] M. Stakić, T. Urošević, Experimental study and simulation of vibrated fluidized bed drying, Chemical Engineering and Processing: Process Intensification, 50 (2011) 428-437.
[15] F.C. Godoi, N.R. Pereira, S.C.S. Rocha, Analysis of the drying process of a biopolymer (poly-hydroxybutyrate) in rotating-pulsed fluidized bed, Chemical Engineering and Processing: Process Intensification, 50 (2011) 623-629.
[16] L. Meili, R.V. Daleffe, M.C. Ferreira, J.T. Freire, Analysis of the Influence of Dimensionless Vibration Number on the Drying of Pastes in Vibrofluidized Beds, Drying Technology, 28 (2010) 402-411.
[17] L.F.G. de Souza, M. Nitz, P.A. Lima, O.P. Taranto, Drying of Sodium Acetate in a Pulsed Fluid Bed Dryer, Chemical Engineering & Technology, 33 (2010) 2015-2020.
[18] V. Bubnovich, C. Villarreal, A. Reyes, Computer Simulation of the Drying of Seeds and Vegetables in a Discontinuous Fluidized Bed, Numerical Heat Transfer: Part A -- Applications, 54 (2008) 255-278.
[19] A. Akhavan, J.R. van Ommen, J. Nijenhuis, X.S. Wang, M.-O. Coppens, M.J. Rhodes, Improved Drying in a Pulsation-Assisted Fluidized Bed, Industrial & Engineering Chemistry Research, 48 (2008) 302-309.
[20] A. Reyes, P. Moyano, J. Paz, Drying of Potato Slices in a Pulsed Fluidized Bed, Drying Technology, 25 (2007) 581-590.
[21] M. Nitz, O.P. Taranto, Drying of beans in a pulsed fluid bed dryer: Drying kinetics, fluid-dynamic study and comparisons with conventional fluidization, Journal of Food Engineering, 80 (2007) 249-256.
[22] A. Reyes, C. Campos, R. Vega, Drying of Turnip Seeds with Microwaves in Fixed and Pulsed Fluidized Beds, Drying Technology, 24 (2006) 1469-1480.
[23] R.V. Daleffe, M.C. Ferreira, J.T. Freire, Drying of Pastes in Vibro-Fluidized Beds: Effects of the Amplitude and Frequency of Vibration, Drying Technology, 23 (2005) 1765-1781.
[24] Z. Li, N. Kobayashi, S. Deguchi, M. Hasatani, Investigation on the Drying Kinetics in a Pulsed Fluidized Bed, JOURNAL OF CHEMICAL ENGINEERING OF JAPAN, 37 (2004) 1179-1182.
[25] T. Kudra, Z. Gawrzynski, R. Glaser, J. Stanislawski, M. Poirier, DRYING OF PULP AND PAPER SLUDGE IN A PULSED FLUID BED DRYER, Drying Technology, 20 (2002) 917-933.
[26] Z. Gawrzynski, R. Glaser, Drying in a Pulsed-Fluid Bed with Relocated Gas Stream, Drying Technology, 14 (1996) 1121-1172.

[27] M. Hasatani, Y. Itaya, K. Miura, DRYING OF GRANULAR MATERIALS IN AN INCLINED VIBRATED FLUIDIZED BED BY COMBINED RADIATIVE AND ONVECTIVE HEATING, Drying Technology, 9 (1991) 349-366.
[28] M.-O. Coppens, J.R. van Ommen, Structuring chaotic fluidized beds, Chemical Engineering Journal, 96 (2003) 117-124.
[29] A.A.H. Drinkenburg, Proceedings of the International Symposium on Fluidization, June 6-9, 1967, Eindhoven, Netherlands University Press, 1967.
[30] G.V. L. Massimilla, G. Raso, A study on pulsating gas fluidization of beds of particles, in: Chemical Engineering Progress Symposium Series, American Institute of Chemical Engineers, 1966, pp. 63.
[31] H.W. Wong, M.H.I. Baird, Fluidisation in a pulsed gas flow, The Chemical Engineering Journal, 2 (1971) 104-113.
[32] X.S. Wang, M.J. Rhodes, Pulsed fluidization—a DEM study of a fascinating phenomenon, Powder Technology, 159 (2005) 142-149.
[33] R. Gupta, A.S. Mujumdar, Aerodynamics of a vibrated fluid bed, The Canadian Journal of Chemical Engineering, 58 (1980) 332-338.
[34] E.R.A. Eccles, A.S. Mujumdar, CYLINDER-TO-BED HEAT TRANSFER IN AERATED VIBRATED BEDS OF SMALL PARTICLES, Drying Technology, 10 (1992) 139-164.
[35] D. Zhang, Hydrodynamics and heat transfer in a pulsed bubbling fluidized bed, in, Dalhousie University (Canada), Ann Arbor, 2005, pp. 214-214 p.
[36] W. Wagner, A. Pruss, International Equations for the Saturation Properties of Ordinary Water Substance. Revised According to the International Temperature Scale of 1990. Addendum to J. Phys. Chem. Ref. Data 16, 893 (1987), Journal of Physical and Chemical Reference Data, 22 (1993) 783-787.
[37] H. Cui, J.R. Grace, Fluidization of biomass particles: A review of experimental multiphase flow aspects, Fluidized Bed Applications, 62 (2007) 45-55.
[38] B. Hao, H.T. Bi, Forced bed mass oscillations in gas–solid fluidized beds, Powder Technology, 149 (2005) 51-60.
[39] H.T. Bi, A critical review of the complex pressure fluctuation phenomenon in gas–solids fluidized beds, Chemical Engineering Science, 62 (2007) 3473-3493.
[40] G.-B. Zhao, Y.-R. Yang, Multiscale resolution of fluidized-bed pressure fluctuations, AIChE Journal, 49 (2003) 869-882.
[41] R. Roy, J.F. Davidson, V.G. Tuponogov, The velocity of sound in fluidised beds, Chemical Engineering Science, 45 (1990) 3233-3245.

[42] Igathinathane, C., Jaya Shankar Tumuluru, S. Sokhansanj, X. Bi, C.J. Lim, S. Melin,E. Mohammad. 2010. Simple and inexpensive method of wood pellets macro-porosity measurement. Bioresource Technology 101 (2010):6528-6537.

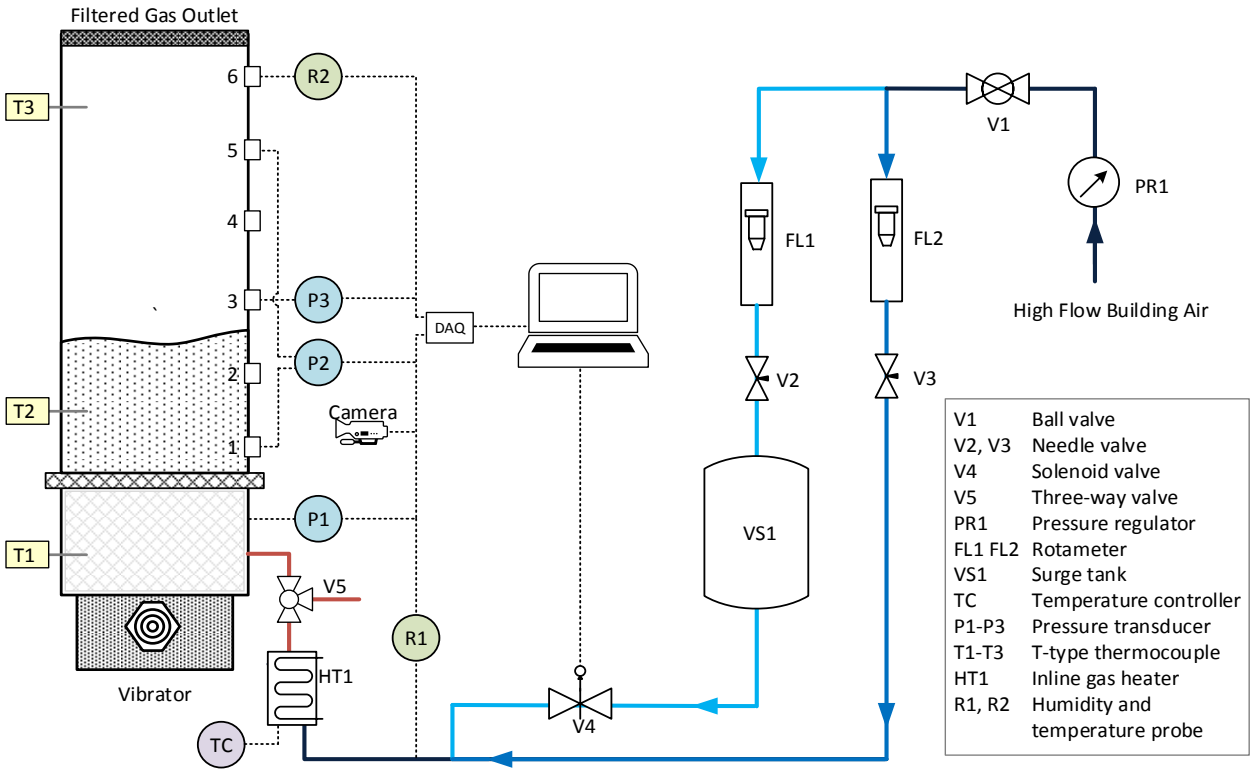

Figure 14. Schematic drawing of the vibrated fluidized bed with pulsed gas flow

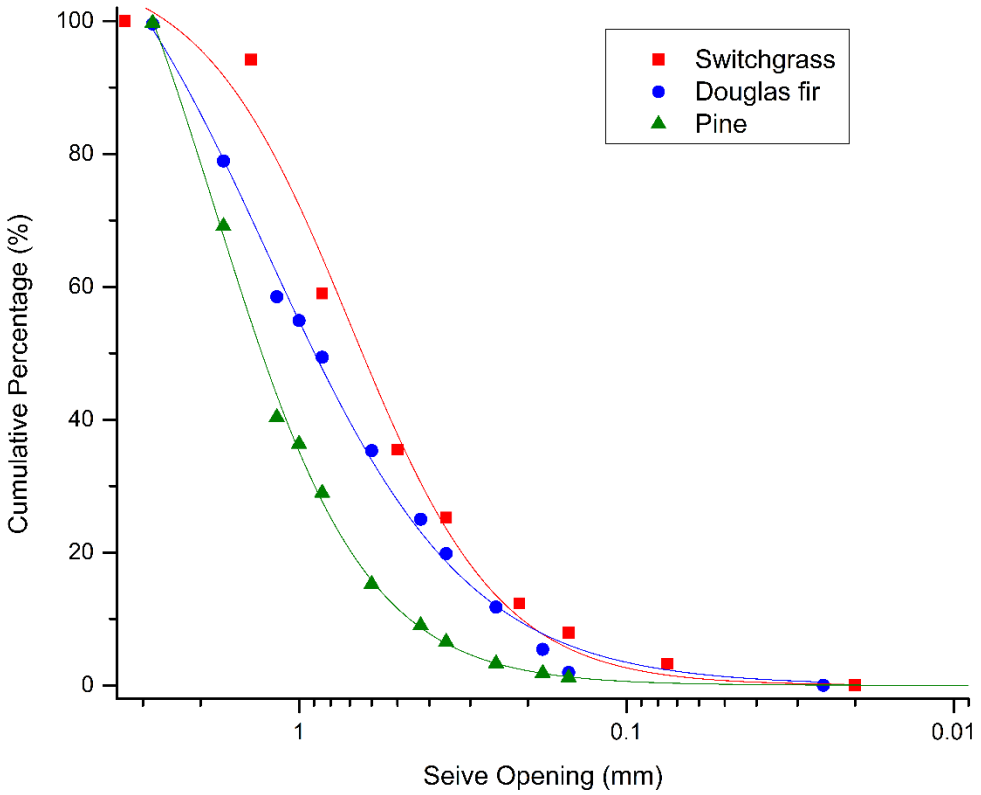

Figure 15. Particle size distribution of bed materials

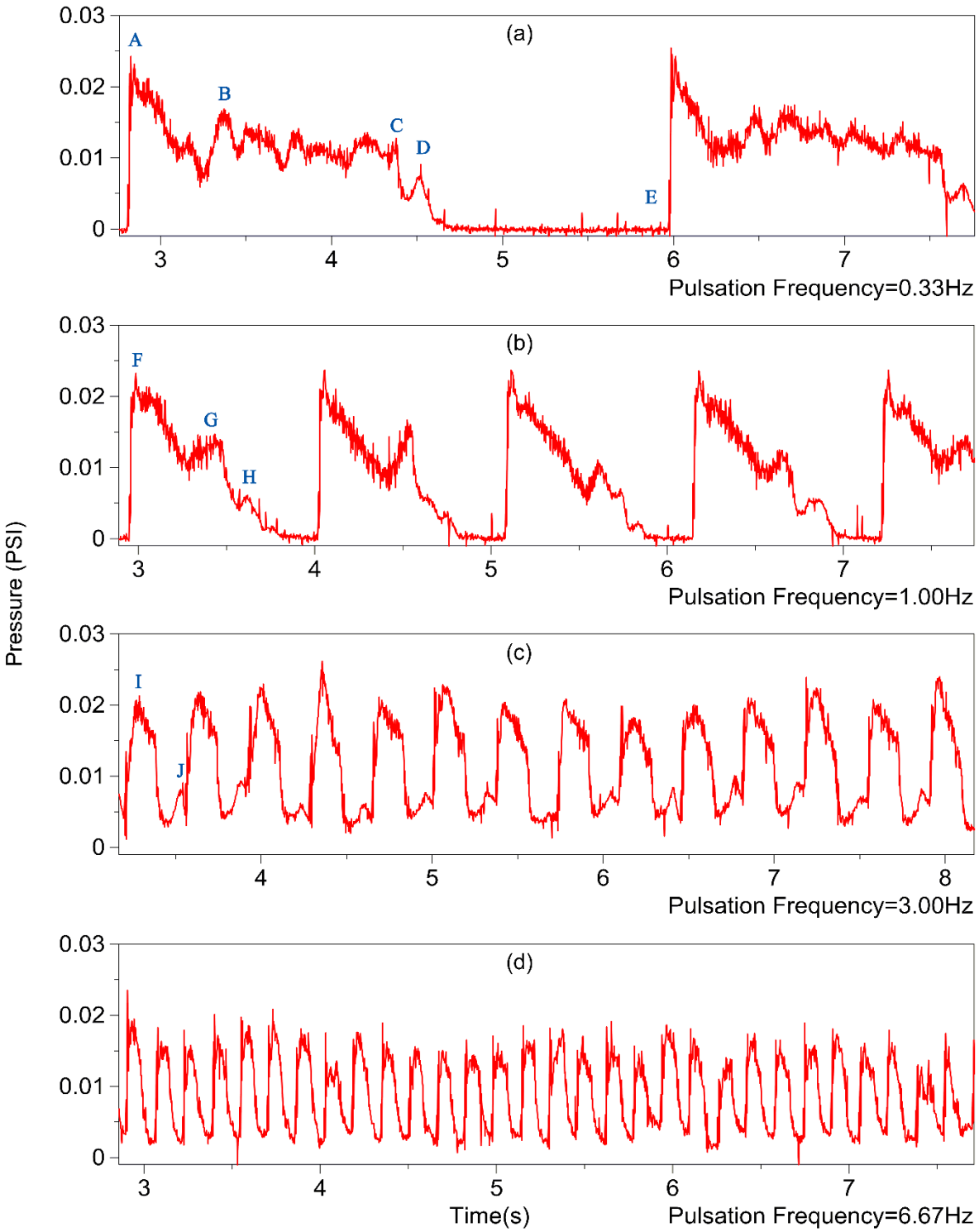

Figure 16. Pressure fluctuations in PVFB at various pulsation frequencies

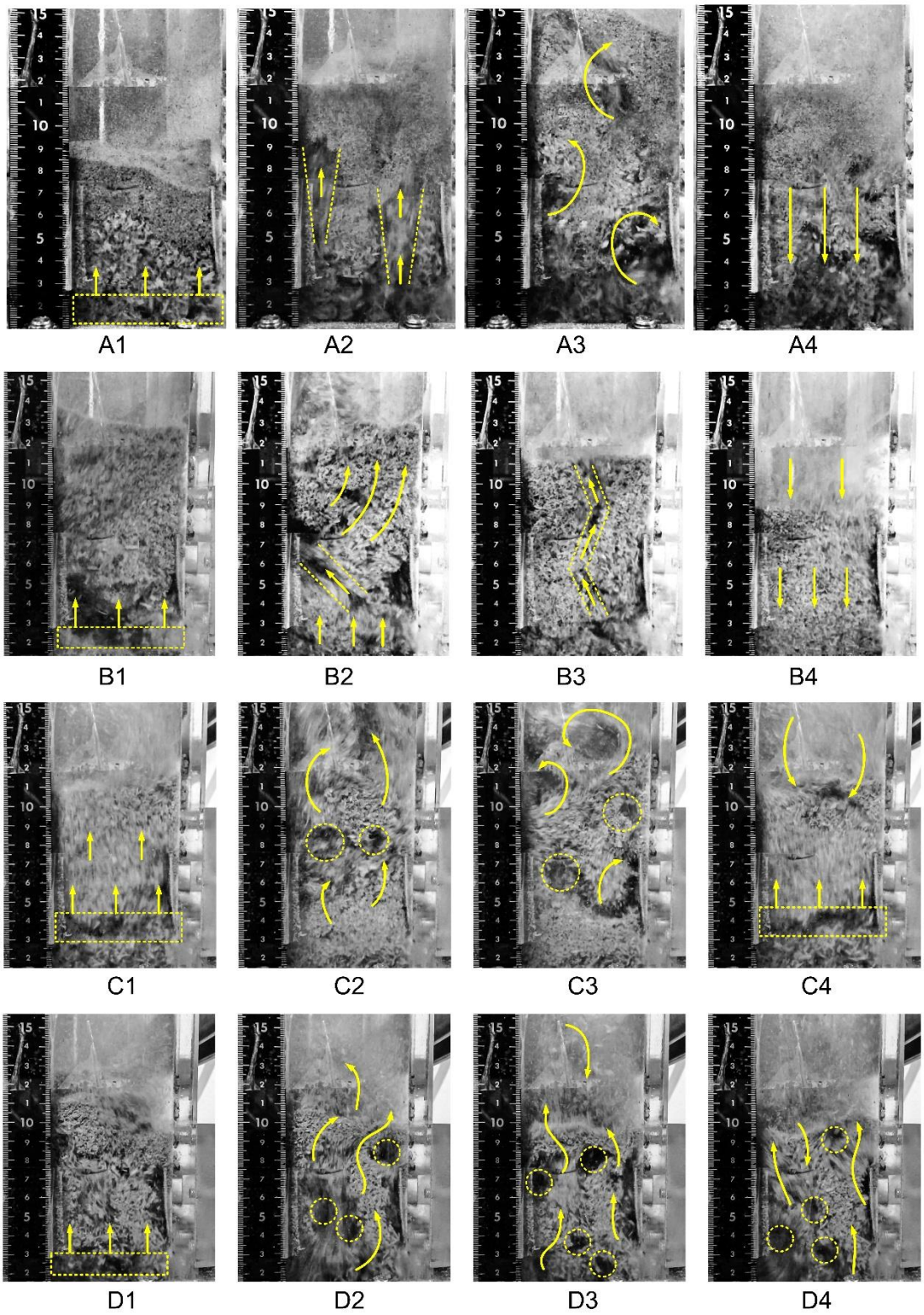

Figure 17. Typical fluid patterns of the bed at various pulsation frequencies. A1-A4 Pulsation frequency = 0.33Hz, B1-B4 1Hz, C1-C4 3Hz, D1-D4 6.67Hz

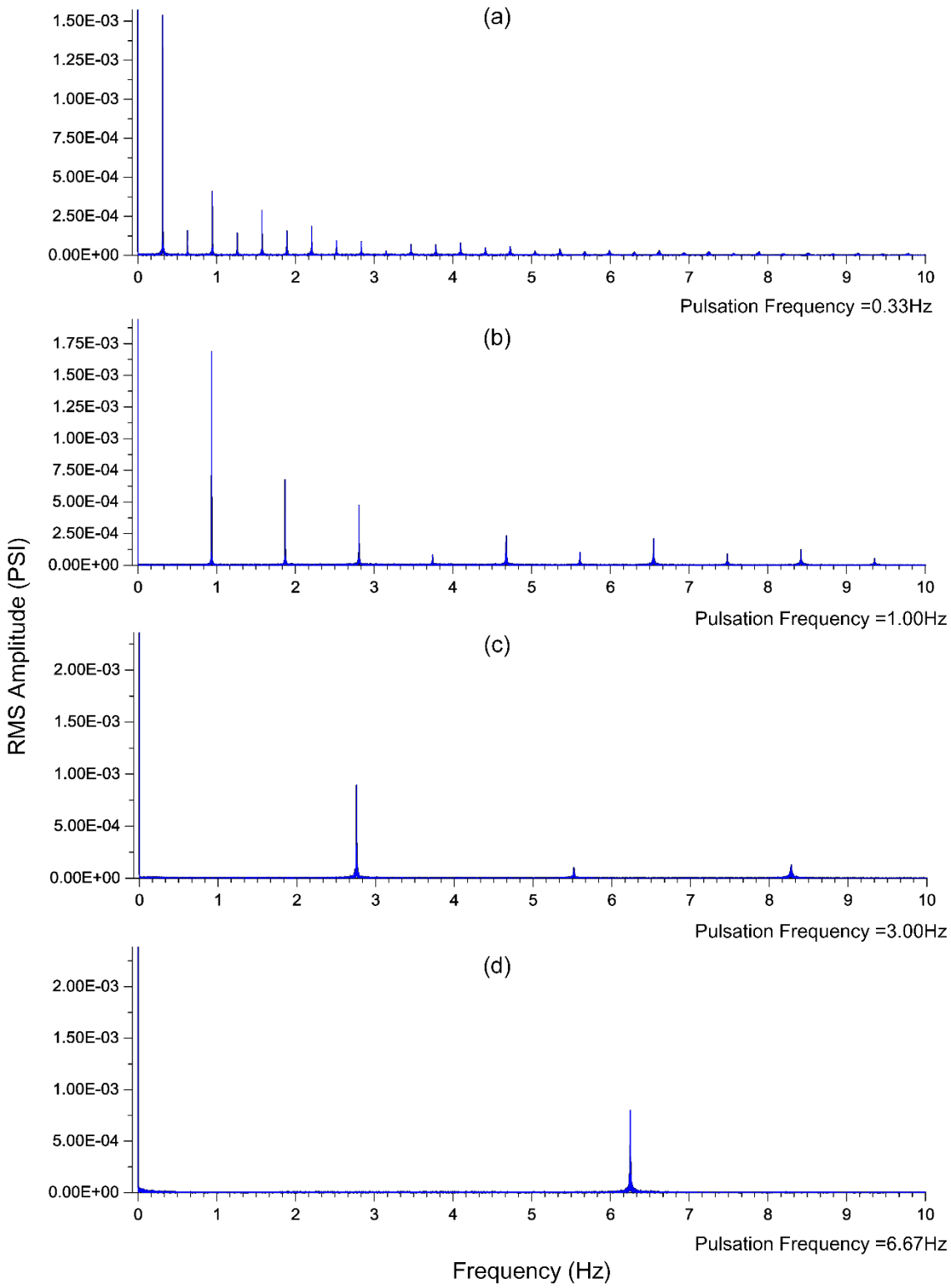

Figure 18. Spectrum analysis of pressure fluctuations at various pulsation frequencies

1

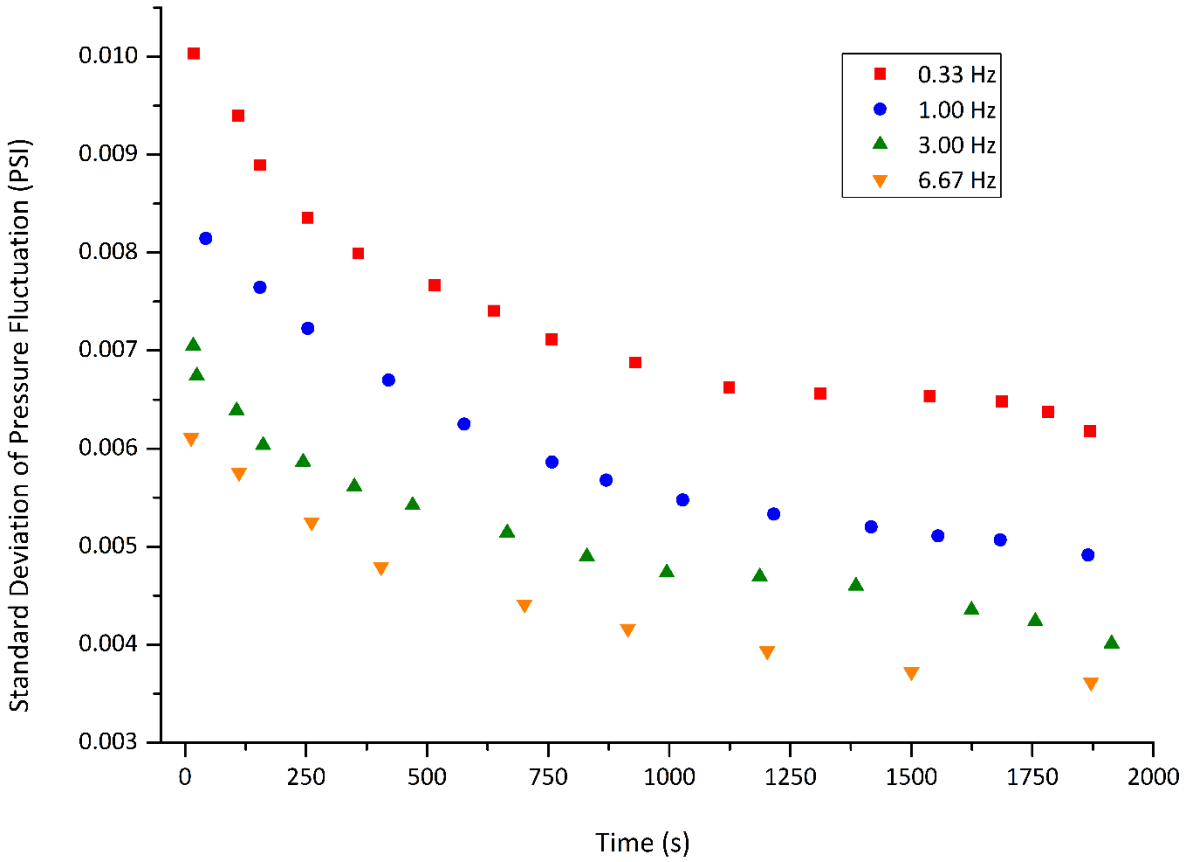

Figure 19. Standard deviation of pressure fluctuations at various pulsation frequencies[S16]

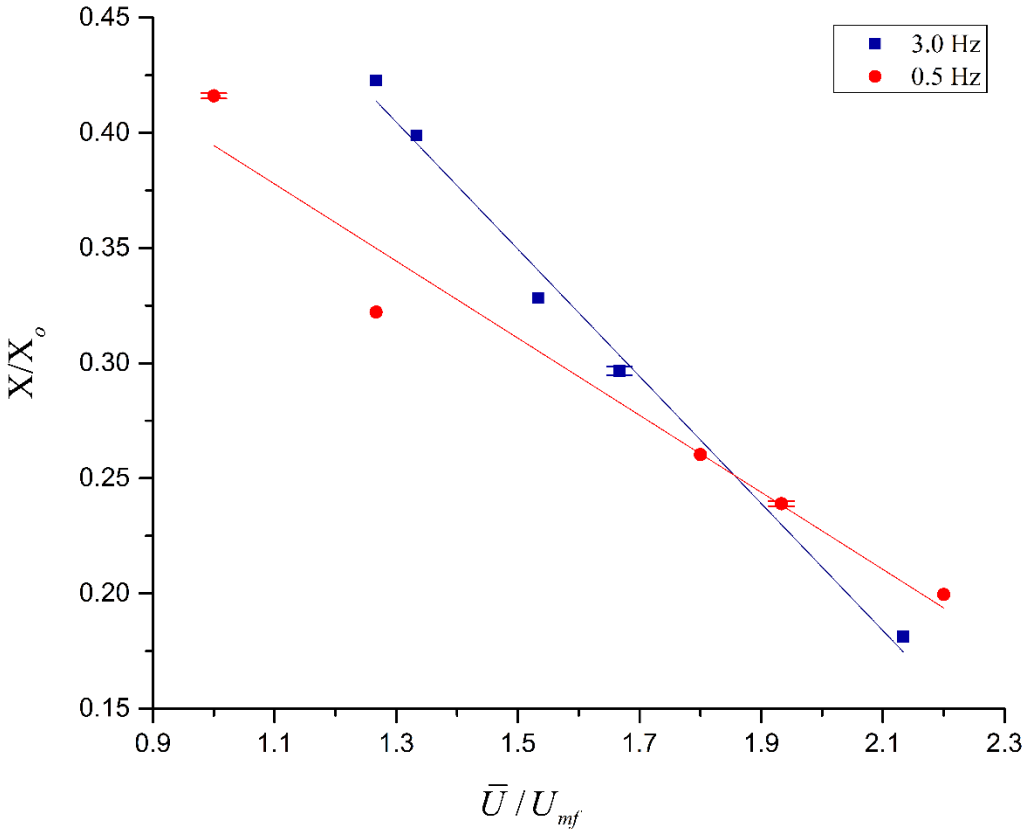

Figure 20. Effect of flow rate on the final moisture content of Douglas fir sawdust after 30 min of drying

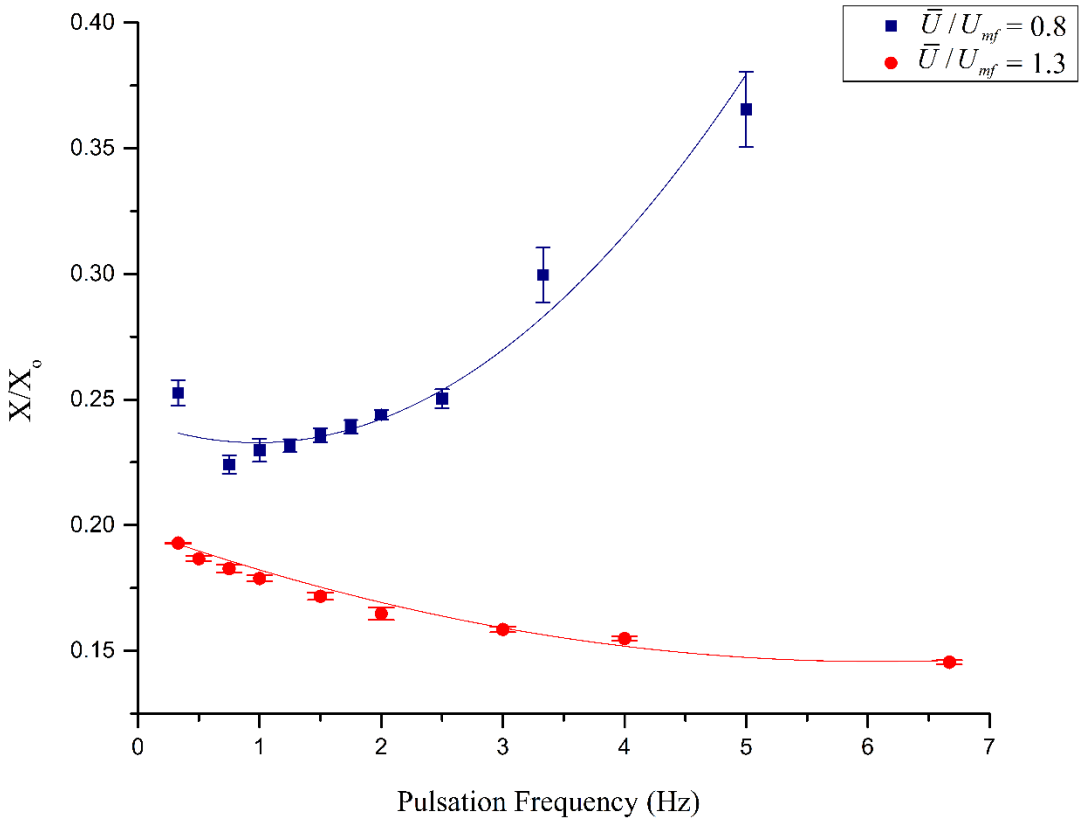

Figure 21. Effect of pulsation frequency on the final moisture content of Douglas fir sawdust after 30 min of drying

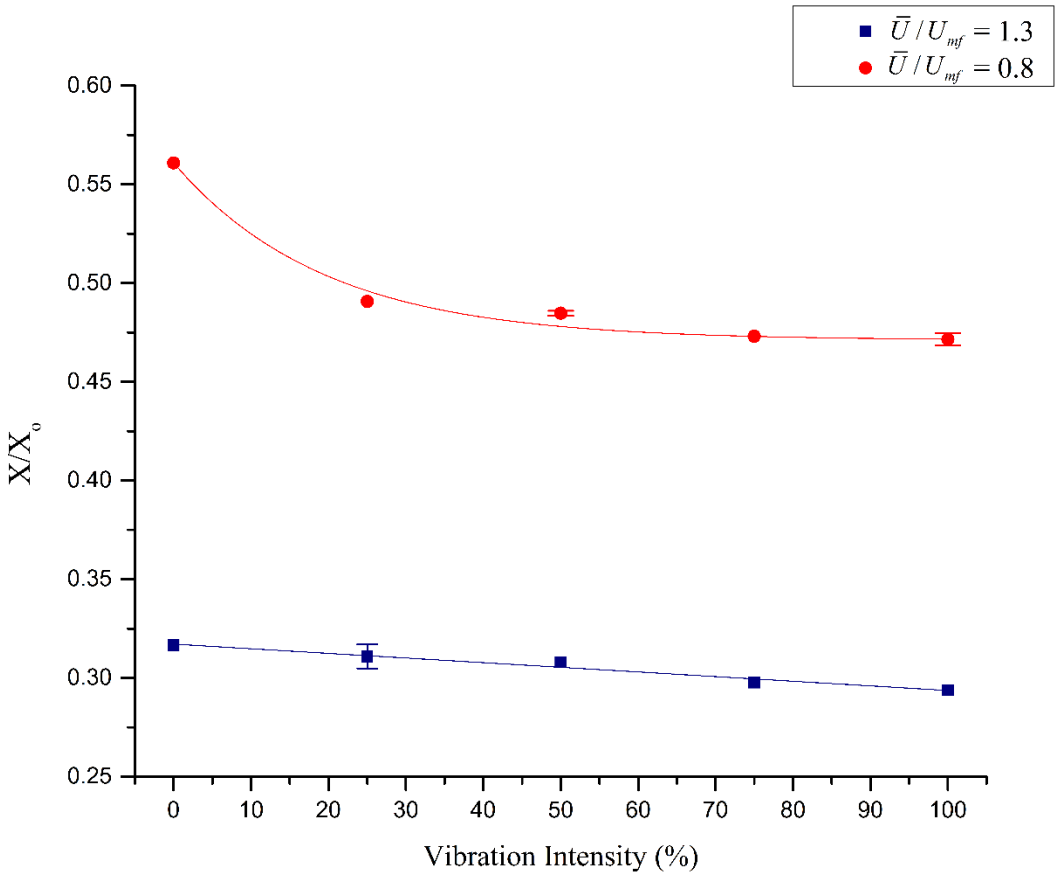

Figure 22. Effect of vibration intensity on drying, Douglas fir sawdust under 1 Hz pulsation frequency

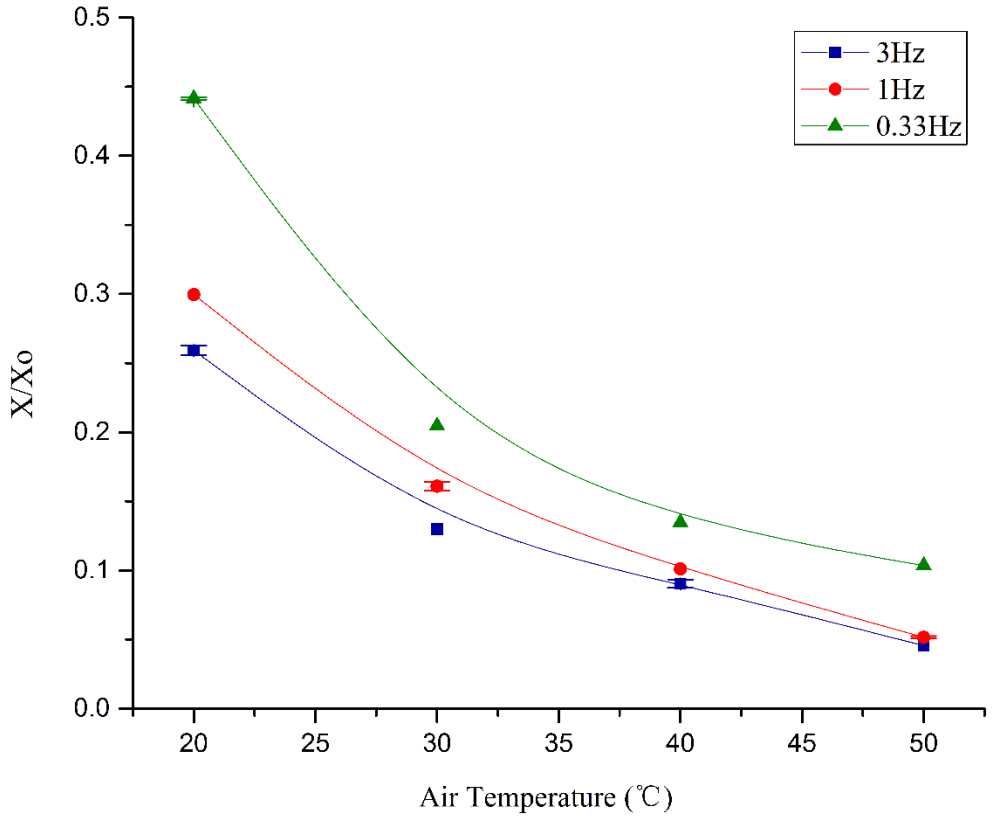

Figure 23. Effect of temperature on the drying of Douglas fir sawdust at various pulsation frequencies, $U/U_{mf}=1.25$

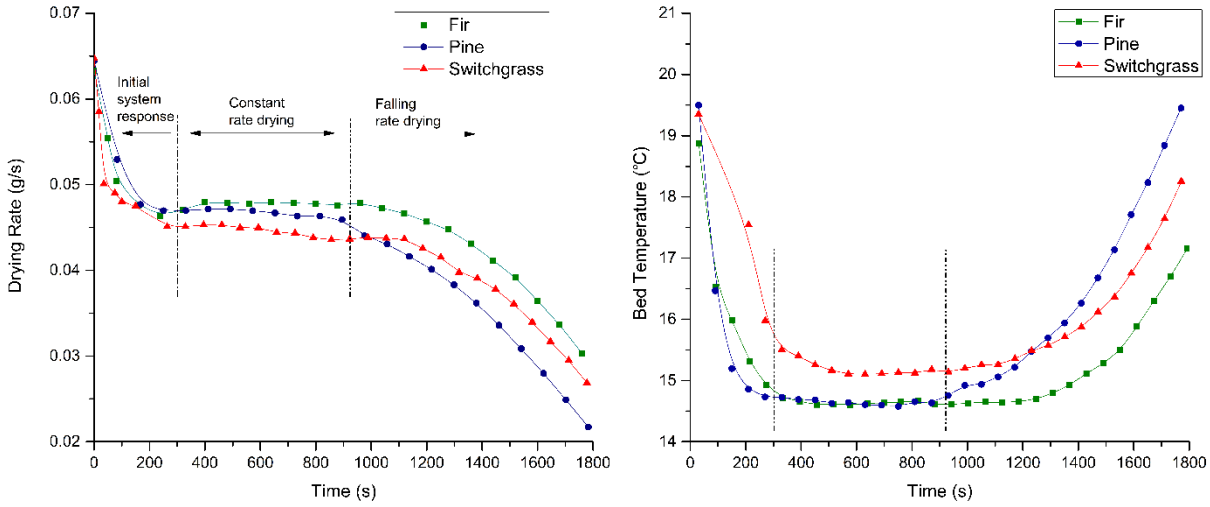

Figure 24. Typical drying curves of three biomass species (a) Drying rate vs. time (b) Bed temperature vs. time

Figure 25. Schematic drawing of the pulsations at different frequencies and flow rates[S17]

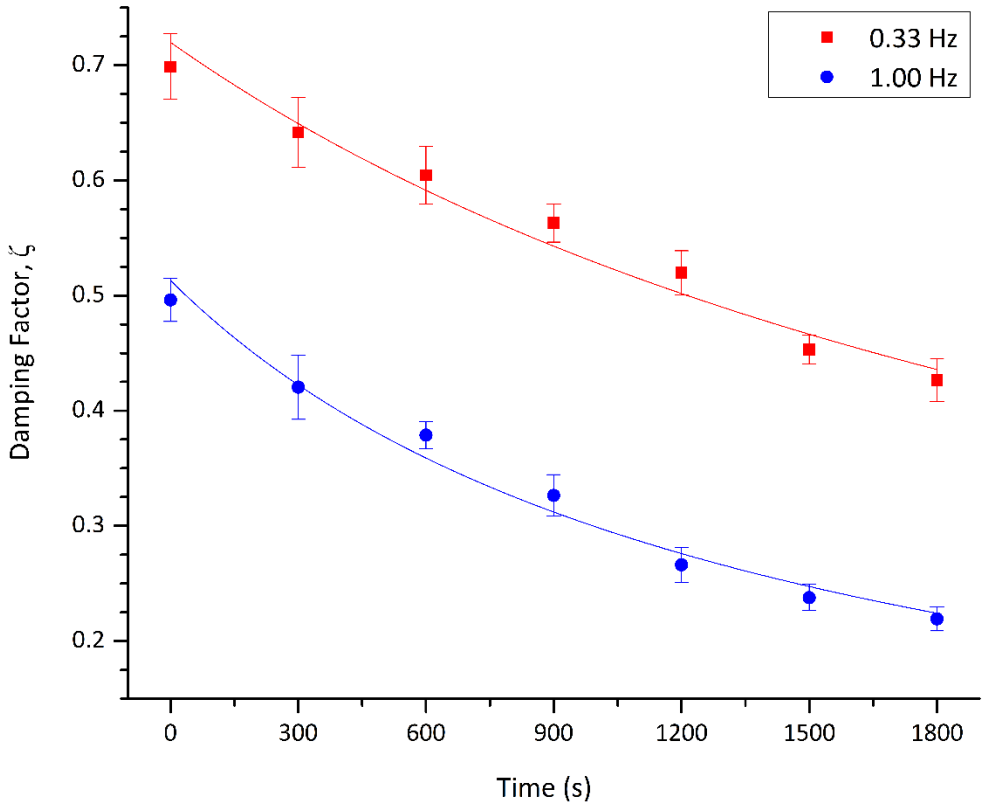

Figure 26.Damping factor of the pulsed fluidized bed during drying of biomass

Table 2. Summary of data acquisition device and acquired signals

Signal Name	Sensor/Actuator	DAQ Model	Sampling Rate
Pressure	Pressure Transducer	MC DAS-08 PCI	400 Hz
Temperature	T-type thermocouple	NI 9214 in cDAQ-9171	20 Hz
Relative humidity with temperature	Vaisala humidity probes	NI USB-6008	10 Hz
Digital Control	Solenoid Valve	NI USB-6009	100 Hz

Table 3. Properties of biomass particles

Biomass species	Bulk density (at 7% moisture content, dry basis), kg/m^3	True density, kg/m^3	Sauter mean diameter, mm	Sphericity
Douglas-fir	164	1375	1.449	0.42
Pine	139	1242	1.469	0.43
Switchgrass	184	1446	0.755	0.65